17. SEVERE PRECIPITATION IN NORTHERN INDIA IN JUNE 2013: CAUSES, HISTORICAL CONTEXT, AND CHANGES IN PROBABILITY

Deepti Singh, Daniel E. Horton, Michael Tsiang, Matz Haugen, Moetasim Ashfaq, Rui Mei, Deeksha Rastogi, Nathaniel C. Johnson, Allison Charland, Bala Rajaratnam, and Noah S. Diffenbaugh

Cumulative precipitation in northern India in June 2013 was a century-scale event, and evidence for increased probability in the present climate compared to the preindustrial climate is equivocal.

The Event: June 2013 Flooding in Northern India. Parts of mountainous northern India—including Himachal Pradesh, Uttarakhand, and Uttar Pradesh—experienced extremely heavy precipitation during 14–17 June 2013 (Fig. 17.1a,b). Landslides, debris flows, and extensive flooding caused catastrophic damage to housing and infrastructure, impacted >100000 people, and resulted in >5800 deaths (Dobhal et al. 2013; Dube et al. 2013; Dubey et al. 2013; Joseph et al. 2014; Mishra and Srinivasan 2013). Subsequent heavy rains on 24–25 June hampered rescue efforts, ultimately leaving thousands without food or shelter for >10 days (Prakash 2013).

Causes of the mid-June precipitation and associated flooding have been analyzed in detail (Dobhal et al. 2013; Dube et al. 2014; Mishra and Srinivasan 2013; Prakash 2013). Anomalously early arrival of monsoon-like atmospheric circulation over India (Fig. 17.1c, Supplementary Figure S17.1a) brought heavy rains to the mountainous regions where snow

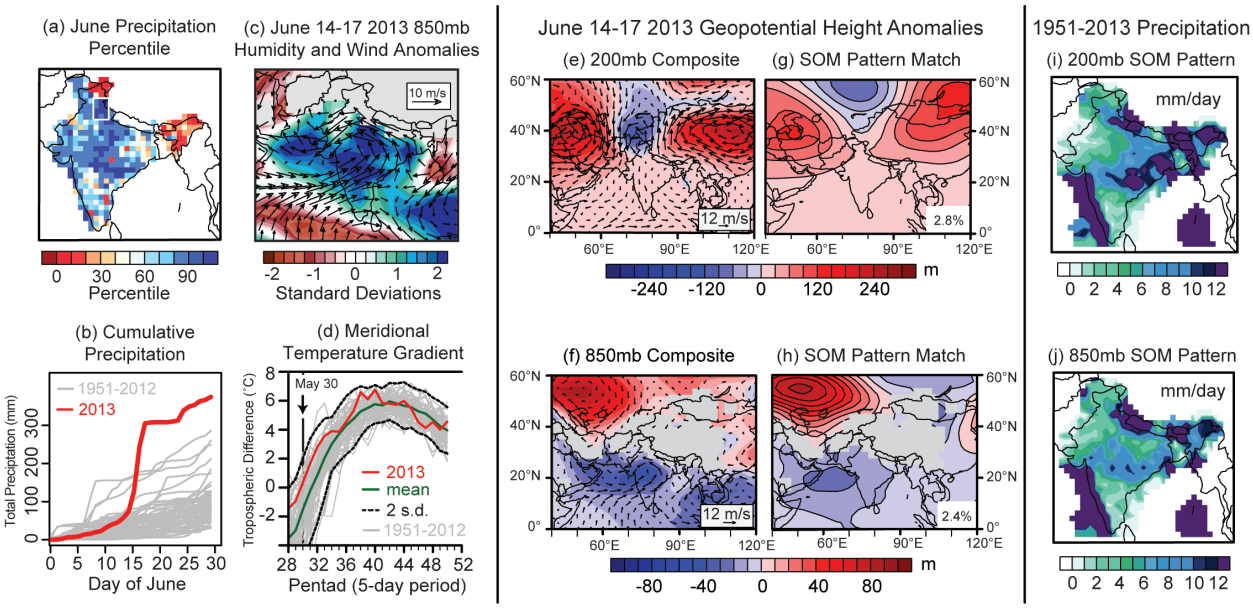

Fig. 17.1. Precipitation characteristics and synoptic environment. (a) June 2013 grid cell cumulative precipitation percentiles relative to June climatology (1951–2012). White box highlights the severe flooding domain (29°–33°N, 77.5°–80°E). (b) Daily cumulative precipitation distribution over the flood domain. (c) 14–17 June 2013 composite lower-level wind and specific humidity anomalies relative to 14–17 June climatology. (d) Climatological and 2013 meridional temperature gradient (MTG), defined as the zonally averaged (52°–85°E) pentad mean tropospheric (200–500 mb) temperature difference between 30°N and 5°N. (e,f) 14–17 June 2013 composite upper- and lower-level wind and geopotential height anomalies relative to the 14–17 June climatology. (g,h) Upper- and lower-atmosphere self-organizing map (SOM) patterns that correspond to 14–17 June 2013. Pattern matches are autonomously selected from 35 SOM nodes, generated from an analysis of all 1951–2013 June days (see Supplemental Materials). (i,j) Composite precipitation for all June days during the 1951–2013 period that were associated with the upper- and lower-level SOM patterns shown in (g) and (h).

cover typically melts prior to monsoon onset (Dube et al. 2014; Joseph et al. 2014). Snow cover in local river basins was ~30% above normal in early June 2013 (Durga Rao et al. 2014). Heavy precipitation led to rapid snowmelt, overwhelming the regional hydrologic system, causing glacial lake outburst floods, and triggering catastrophic mass wastage events (Andermann et al. 2012; Dubey et al. 2013; Durga Rao et al. 2014; Prakash 2013; Siderius et al. 2013).

The upper- and lower-level synoptic conditions in early and mid-June supported the anomalously early monsoon-like circulation (Supplementary Fig. S17.1a) and excessive precipitation in northern India (Fig. 17.1a,b). In the upper atmosphere (200 mb), a persistent anticyclonic anomaly formed over Central Asia (Fig. 17.1e). This upper-level blocking pattern guided mid-to-high-latitude troughs southward, thereby facilitating the advection of relatively cold, dry, high-potential-vorticity air to the upper levels of the atmosphere over northern India (Joseph et al. 2014). In the lower atmosphere (850 mb), low-pressure systems formed over both the northern Bay of Bengal and the northern Arabian Sea (Joseph et al. 2014), with the Bay of Bengal system moving inland over central India and persisting for the duration of the event (Fig. 17.1f). Low-level convergence associated with these systems and a stronger-than-normal Somali Jet facilitated anomalous moisture advection to the Indian subcontinent (Fig. 17.1c). These co-occurring upper- and lower-level dynamics are consistent with a convectively unstable atmosphere (Hong et al. 2011; Ullah and Shouting 2013; Wang et al. 2011), which, when combined with orographic forcing from the surrounding northwestern Himalayan terrain, create an environment ripe for intense mesoscale convection (Houze et al. 2011).

In this study, we analyze the dynamics of this event within the context of the historical and preindustrial climates.

Historical context. We contextualize June 2013 precipitation using the Indian Meteorological Department (IMD) 1951–2013 1° × 1° gridded dataset (Rajeevan et al. 2010), with the caveat that the rain gauge network in the region could have changed over this period. Cumulative June precipitation exceeded the 80th percentile over much of central and northern India, and it exceeded the maximum quantile over a majority of the flood region (Fig. 17.1a). From 14 to 17 June, this domain (29°–33°N, 77.5°–80°E) received four-day total precipitation that was unprecedented in the observed record (Fig. 17.1b), with the heaviest day (16 June) exceeding the previous one-day June maximum by 105% (Supplementary Fig. S17.2). Consequently, the flood region recorded the highest total accumulated June precipitation in the 1951–2013 record, with the previous maximum June total equaled by 17 June and exceeded by 31% by the end of the month (Fig. 17.1b).

Monsoon dynamics and thermodynamics were also unusual relative to June climatological norms. The monsoon onset date is closely associated with the reversal of the zonally averaged (52°–85°E) meridional tropospheric (500–200 mb) ocean-to-continent (5°–30°N) temperature gradient (Ashfaq et al. 2009; Webster et al. 1998), and with the vertical easterly zonal wind shear between 850 mb and 200 mb averaged over 0°–30°N and 50°–90°E (Li and Yanai 1996; Webster et al. 1998; G. Wu et al. 2012; Xavier et al. 2007). The 2013 meridional temperature gradient (MTG) reversal dates were among the earliest on record (1951–2013, Fig. 17.1d) and the vertical easterly wind shear was stronger than normal during early-June (Supplementary Fig. S17.1b). The early MTG reversal resulted from anomalously high land temperatures (~2 standard deviations; Supplementary Fig. S17.1c,d), which co-occurred with record-low Eurasian snow cover (NOAA 2013). In addition, as a result of the early monsoon-like circulation, low-level atmospheric humidity exceeded 2 standard deviations above the climatological 14–17 June mean (Fig. 17.1c).

Synoptic conditions were likewise extremely rare for mid-June. We categorize the occurrence of upper- and lower-level daily June atmospheric patterns in the National Centers for Environmental Prediction (NCEP) R1 reanalysis using self-organizing map (SOM) cluster analysis (Borah et al. 2013; Chattopadhyay et al. 2008; Hewitson and Crane 2002; Johnson 2013; Kohonen 2001; see Supplemental Materials). SOM analyses reveal persistent upper-level blocking patterns from 10 to 17 June and lower-level troughing patterns from 11 to 17 June (Supplementary Fig. S17.2). Additionally, the upper- and lower-level patterns (Fig. 17.1g,h) that persisted during the core of the event (14–17 June) are each historically associated with heavy precipitation over northern India (Fig. 17.1i,j). Although occurrence of the core-event upper-level pattern is not rare for June (median frequency of occurrence), the 850-mb pattern is much less common (<6 percentile frequency of occurrence). Further, mid-June 2013 was the only instance that the core-event upper- and lower-level patterns co-occurred in June during the 1951–2013 period. The atmospheric

configuration associated with the unprecedented mid-June extreme precipitation, therefore, appears to also have been unprecedented.

We note that this configuration is not necessarily unprecedented later in the monsoon season. For example, the co-occurrence of upper-level blocking with tropical moisture advection is similar to the conditions identified during the July 2010 Pakistan floods and during heavy precipitation events that occur during the core monsoon season (Hong et al. 2011; Houze et al. 2011; Lau and Kim 2011; Ullah and Shouting 2013; Webster et al. 2011).

Quantifying the probability of a 2013-magnitude event. In quantifying the probability of a 2013-magnitude event, we restrict our focus to the June 2013 total precipitation. We select the monthly scale extreme rather than the daily scale extreme because both the extreme magnitude of this event relative to the observed distribution of four-day June totals and the limited ability of climate models to accurately simulate the daily scale extremes make the problem intractable at the daily scale. Therefore, hereafter, "a 2013-magnitude event" refers to the total June rainfall, which in June 2013 was the most extreme on record (Fig. 17.1b).

Given the rarity of the event in the observed record (Fig. 17.2a), we fit a Pareto (heavy-tailed) distribution to the 1951–2012 observations of spatially averaged (area-weighted average) rainfall over the selected domain (Fig. 17.2a; Supplementary Fig. S17.3a). From the Pareto distribution, we estimate the sample quantile (Q_o) and return period (R_o) of the June 2013 total precipitation in the present climate (see Supplemental Materials). We find that the 2013 event exceeds the 99th percentile in the observed distribution (Q_o = 99.1th quantile), yielding a return period of 111 years (Fig. 17.2a). Because the Pareto is a heavy-tailed distribution, extreme events are less likely to be found anomalous, and, thus, the corresponding return period can be considered a lower bound.

Next, we assess the influence of anthropogenic forcings on the likelihood of extreme June precipitation using the historical (20C) and preindustrial (PI) simulations from the CMIP5 climate model archive (Taylor et al. 2012). We use the Kolmogorov–Smirnov (K-S) goodness-of-fit test to identify the models that most closely simulate the observed distribution of the area-weighted average June total precipitation over the impacted region (Fig. 17.1a). (To control for the mean bias in the models, we first re-center each model's distribution so that the model mean matches the observed mean.) Because the simulated change in likelihood of extremes can be heavily influenced by biases in the simulated distribution, we restrict our analyses to 11 models whose K-S value exceeds 0.2 (Supplementary Fig. S17.3b), ensuring a comparatively good fit of the overall distribution, including in the tails. Among these 11 models that pass this goodness-of-fit criterion, 4 show greater mean and variability of June precipitation in the 20C simulations (Fig. 17.2b). However, 7 of the 11 show increased exceedance of the PI 99th percentile value (Fig. 17.2c), suggesting increased probability of extremely high June precipitation in the current climate. This result is consistent with studies that indicate an increase in extremes primarily from increased atmospheric-moisture availability (Allan and Soden 2008; O'Gorman and Schneider 2009).

Next, we use Pareto distributions to estimate the return period of the June 2013 total precipitation in the 20C and PI simulations. To control for the variability-bias in the models, we first determine the magnitude of the 111-year event (Q_o= 99.1th quantile) in the fitted 20C distribution (Pr_H), and then determine the quantile (Q_{PI}) corresponding to Pr_H in the fitted PI distribution (see Supplemental Materials; Supplementary Fig. S17.3c). Further, we quantify the uncertainty in these likelihood estimates (Q_o/Q_{PI}) using the bootstrap (Fig. 17.2d). We find that 5 of the 11 models show >50% likelihood that the extreme June total precipitation has higher probability in the 20C climate. In addition, of the three models that have high *p*-values from the K-S test (> 0.8) and similar sample sizes in the 20C and PI populations (Fig. 17.2d), two suggest >50% likelihood that the extreme June total precipitation has higher probability in the 20C climate, and the third model suggests ~50% likelihood. Further, the model with the largest 20C ensemble (Centre National de Recherches Meteorologiques Coupled Global Climate Model; CNRM-CM5) demonstrates a ~50% likelihood that the probability of the extreme June total precipitation has at least doubled in the 20C climate. CNRM-CM5 also has the highest skill in simulating the summer monsoon precipitation and lower-level wind climatology (Sperber et al. 2013).

Conclusions. Our statistical analysis, combined with our diagnosis of the atmospheric environment, demonstrates that the extreme June 2013 total precipitation in northern India was at least a century-scale event. Precise quantification of the likelihood of the event in the current and preindustrial climates is limited by the relatively short observational record

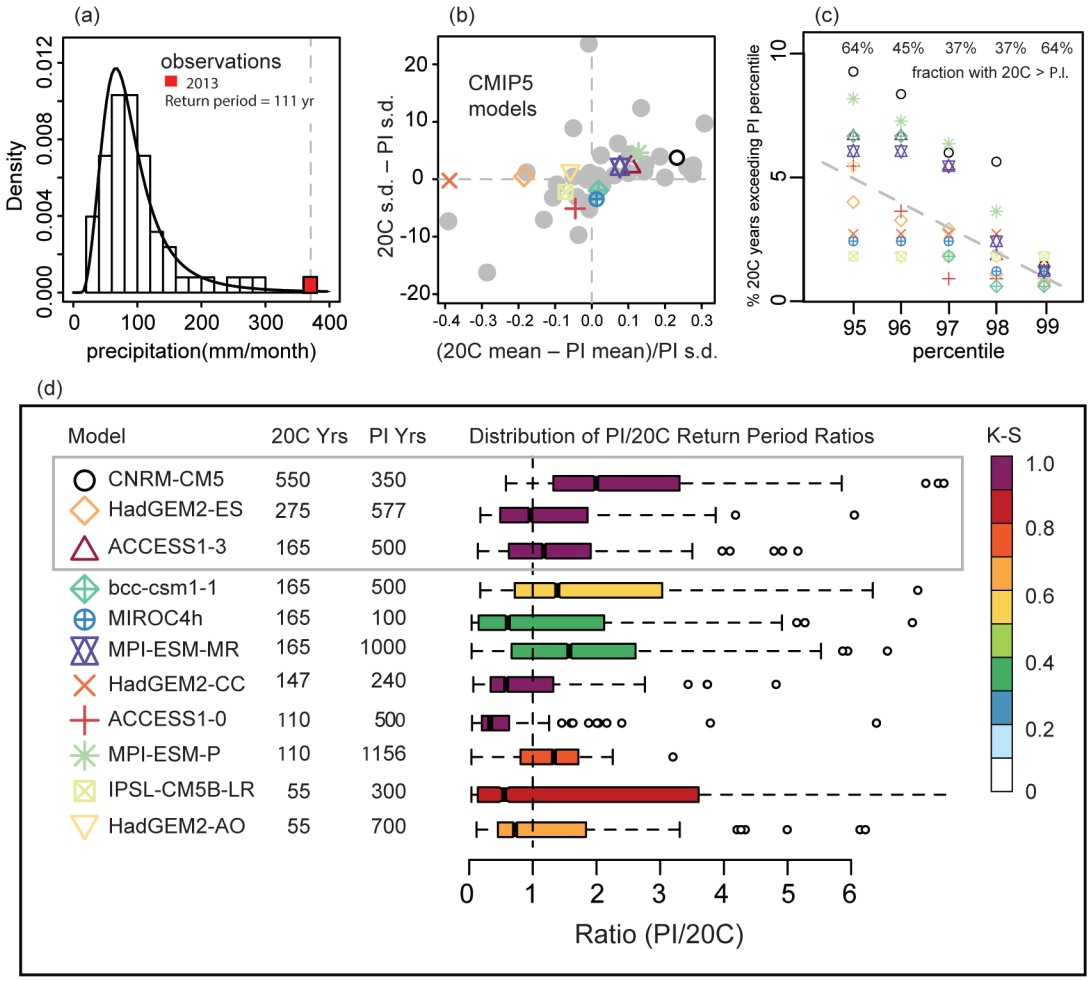

Fig. 17.2. Extreme precipitation statistics in the current and preindustrial climates. (a) Probability density function of the Pareto-fitted observed cumulative-June precipitation distribution (black line; 1951–2012), and probability of occurrence of the June 2013 cumulative precipitation magnitude in this distribution (red). The return period of the June 2013 magnitude in the observed distribution is indicated on the plot. (b) Change in mean and standard deviation of precipitation between the CMIP5 historical (20C) and preindustrial (PI) simulations. Gray dots represent all available CMIP5 models and colored symbols represent AI models that meet the Kolmogorov–Smirnov (K-S) goodness-of-fit test criteria (*p* value > 0.2). (c) Percent of years in the 20C simulations of AI models that exceed the respective PI quantiles of the AI models. The numbers on the plot indicate the fraction of AI models that exceed the PI quantiles in the 20C simulations. (d) Box plot representing the distribution of ratios of the return period of a June 2013 magnitude event in the PI and 20C simulations, calculated using the bootstrap. The lines in the boxes represent the median of the distribution for each model. The bounds of the boxes represent the 25th and 75th percentiles. The whiskers extend to the edges of 1.5×interquartile range, and points outside of those bounds are shown individually. The number of years indicated for the 20C Yrs and PI Yrs columns are the total years available from all realizations within each scenario. The color bar corresponding to the box plot indicates *p* values from the Kolmogorov–Smirnov test.

and by the resolution and ensemble size of the small subset of models that credibly simulate the seasonal rainfall distribution over northern India. Indeed, an attempt to quantify the probability of the unprecedented four-day precipitation total would present even greater analytical challenges. However, despite these limitations, our analyses of the observed and simulated June precipitation provide evidence that anthropogenic forcing of the climate system has increased the likelihood of such an event, a result in agreement with previous studies of trends in rainfall extremes in India (Goswami et al. 2006; Krishnamurthy et al. 2009; Ghosh et al. 2012; Singh et al. 2014).